Geophys. J. Int. (2008) **173,** 79–91 doi: 10.1111/j.1365-246X.2007.03707.x

Implication of kinematic dynamo studies for the geodynamo

David Gubbins

School of Earth and Environment, University of Leeds, Leeds LS2 9JT, *UK. E-mail: gubbins@earth.ac.uk*

Accepted 2007 December 3. Received 2007 December 1; in original form 2006 October 3

SUMMARY

In the kinematic dynamo problem Maxwell's equations are solved for the magnetic field given a prescribed fluid velocity. Although no dynamic equations are involved, it does provide an accurate link between the magnetic field and fluid velocity and can therefore be used to infer something about the flow underlying the observed geomagnetic field. In this sense it complements the commonly used frozen-flux theory for inverting secular variation for core flow, in which electrical diffusion is neglected, and can be used to show up some of the strengths and weaknesses of the frozen-flux approximation. It might be thought that kinematic models have been superceded by dynamic models that include the momentum and heat equations, but this is not the case. Even the biggest numerical simulation cannot approach the correct parameters for the Earth's core, and the classes of flows that result are, in fact, quite restricted as well as being too complex for simple physical interpretation. A variety of simple flows have been studied for dynamo action; of particular interest here are a broad class of flows, based loosely on extensions of the early simple choice of Bullard & Gellman and to some extent representative of what might be generated by convection in the Earth's rapidly rotating core: this paper reviews the implications of the solutions for geomagnetism. The non-axisymmetric flows mimic convection rolls in a rotating sphere, the axisymmetric poloidal flows describe meridional circulation, a likely secondary flow, and the axisymmetric toroidal flow is a simple differential rotation. Helicity, which seems to be important for dynamo action, is related to spiralling of the rolls. Dipole, rather than quadrupole, fields are preferred when spiralling is eastward and differential rotation westward at the surface. Magnetic flux tends to be concentrated at stagnation points of the flow, and dynamo action fails when this concentration becomes so intense that steep gradients develop so as to enhance energy loss by diffusion. On the surface these stagnation points are centres of downwelling that concentrate vertical flux. Flux concentration plays an important role in determining the magnetic field's symmetry: for example, concentration of vertical flux in high latitudes favours dipolar fields while concentration near the equator, where dipole symmetry requires a change of sign, favours quadrupole symmetry. Steady fluid flow can only produce steady or oscillatory solutions to the kinematic problem at onset of instability. Steady solutions are preferred in three dimensions, in contrast to predictions of axisymmetric mean-field dynamo theory, where oscillatory solutions are the most common. Oscillatory solutions are preferred when poloidal and toroidal field coincide, which is unlikely to happen in the Earth because poloidal field is concentrated at high latitudes around the tangent cylinder while the toroidal field is probably strongest in mid-latitudes. Geomagnetic reversals are not oscillatory in nature and, therefore, require time-dependent flow, but kinematic examples show that only a tiny change in flow is needed to produce a realistic geomagnetic reversal. Linear modes of the induction equation of all symmetries are beginning to guide work on the dynamics of the geodynamo.

Key words: Dynamo: theories and simulations; Geomagnetic excursions; Reversals: process, time scale, magnetostratigraphy.

1 INTRODUCTION

The geomagnetic field is generated by a dynamo process operating in the liquid iron core. We advance our understanding of this process by studying simple models of convection of electrically conducting fluid in a rapidly rotating sphere surrounded by an electrical insulator. Although the basic features of the geomagnetic field seem simple—a steady dipole aligned with the spin axis—the dynamo theory is not simple and mostly involves numerical modelling. Complexity is necessitated because a homogeneous sphere of conducting fluid must regenerate magnetic field by the same mechanism as an engineering dynamo, which is multiply connected with a complicated geometry. Several results, such as Cowling's theorem which states that no dynamo can generate a magnetic field that is symmetric about an axis, can be lumped roughly into the statement that 'nothing simple works'. This is unsatisfactory: theories should be elegant but we persist with the dynamo theory because 'nothing else works'.

Early studies focused on the basic question of whether any homogeneous sphere of fluid can generate a magnetic field by addressing the kinematic problem in which the fluid velocity is specified and Maxwell's equations are solved for the magnetic field (Elsasser 1946; Bullard & Gellman 1954; Backus 1958; Herzenberg 1958). Dynamo action is declared if the magnetic energy persists indefinitely. In practice, this usually involves solving for the fastest growing mode of the linear induction equation in the form $\boldsymbol{B} \exp pt$ and searching for $\Re(p) \geq 0$. Recently, Livermore & Jackson (2004a) have introduced a different approach based on the transient growth of magnetic energy, M. If M decays with time initially for all candidate magnetic fields the system is stable; an initial growth of M may indicate instability or a transient that ultimately decays. Thus $\Re(p) < 0$ is a necessary condition for *stability* while $\mathrm{d}M/\mathrm{d}t > 0$ is a necessary condition for *instability*. The distinction becomes important when considering time-dependent flows or turbulent flows in which only the statistical properties of the flow are known. The eigenvalue method for determining linear stability breaks down in these cases (except in the case of time-periodic flows, see Section 3.3.2) but the energy method still gives information about possible dynamo action. Transients that grow initially but then decay under induction by one steady flow may continue to grow when the flow changes at a later time, giving dynamo action when linear stability analysis of individual snapshots of the flow find only decaying modes at every stage. Backus' early dynamo worked in this way (Backus 1958), but the idea of using time-dependent flows was not revisited until recently.

Progress on the dynamics was made through simplified studies of rotating convection, first without and then with an imposed magnetic field, avoiding the need for the system to generate its own magnetic field (e.g. Roberts 1968; Busse 1970; Zhang 1999). Eventually computer power grew to the point when it became possible to explore fully self-consistent dynamo models by solving the coupled equations of momentum, heat, and induction (Zhang & Busse 1990; Glatzmaier & Roberts 1995; Olson *et al.* 1999; Jones 2000). These models involve disarmingly few input parameters: measures of the heating (Rayleigh number), rotation (Ekman number), diffusion (Prandtl numbers) and the boundary conditions, but Earth-like values remain beyond foreseeable computer power. Even simplified choices of parameters yield magnetic fields that are quite Earth-like; unfortunately they are also chaotic with considerable spatial complexity and are, therefore, hard to understand.

In this paper, I review results for the kinematic dynamo problem and their implications for the geodynamo. This return to kinematics needs some justification in view of the current success of dynamic models. There are a number of advantages.

(i) It complements work on core flows using the frozen flux hypothesis. The induction equation connects the magnetic field to the fluid velocity in the core. This is central to using geomagnetic observations to infer core flow and understand the dynamics. The usual approach to finding core flow is to neglect diffusion and use Alfvén's theorem of frozen-in magnetic field to determine core motion from secular variation (Roberts & Scott 1965). This approximation, almost by definition, eliminates the slow, steady flows responsible for generating the magnetic field because the dynamo is a balance of diffusion and advection (Love 1999). The frozen-flux approximation is valid only if the flow varies on a timescale that is longer than that of the magnetic field but shorter than the diffusion time (Braginsky & Le Mouël 1993; Gubbins & Kelly 1996; Gubbins 1996). Diffusion must be included if we are to determine the component of core flow that remains steady for a magnetic diffusion time (25 kyr) or longer, and probably for some historical secular variation events as well.

It is now possible to examine the accuracy of the frozen flux approximation using synthetic SV data obtained from dynamic models; Rau *et al.* (2000) have done this and found the method reproduced the surface flow adequately; Aubert *et al.* (2007) have also used output from dynamic dynamo calculations in a core motion study. This does not mean, however, that the method will work for the Earth. Current geodynamo models are a long way from reality because they employ parameter values that are very different from those of the Earth. While they reproduce some aspects of geomagnetic behaviour surprisingly well, they do not reproduce all behaviour faithfully. Most importantly in the present context they rarely, if ever, produce the kind of flux expulsion now underway in the Southern Hemisphere, which is the very feature showing present departure from frozen flux in the Earth. This restriction on the parameter values that can be explored numerically produces a rather restricted class of flows that may be unrepresentative of the Earth. The key to validity of frozen flux lies in having a rather precise set of timescales, with the field changing rather rapidly on the diffusion timescale. Dynamic models are necessarily run at high Ekman number and high Rayleigh number, putting them into a chaotic regime that would favour frozen flux. Since only the induction equation is involved in determining the evolution of the field and its inversion for core flow by frozen flux, all the dynamic equation does is to restrict the possible flow. It is better, therefore, to examine the validity of frozen-flux theory using a kinematic approach with plausible flows.

(ii) Long-time integrations are unnecessary. Solutions of the induction equation with steady flow vary exponentially with time and a positive real part to the exponent guarantees dynamo action. This is a distinct computational advantage over non-linear dynamo simulations that can only demonstrate dynamo action by time integration. The kinematic approach loses much of its attraction when the flow is time dependent because then time stepping is also needed. An exception is the study of time-periodic flows, when the magnetic field varies with time as an exponential multiplied by a periodic function with the same period as the velocity (Willis & Gubbins 2004).

(iii) The induction equation must be satisfied by any dynamo. Solutions are relevant if the fluid flow also satisfies the dynamical equations. Finding flows that produce Earth-like magnetic fields and then determining the dynamics that might produce them is a valid, observation-led approach. A good example of this is the concentration of magnetic flux by downwelling. This kinematic result (Hutcheson & Gubbins 1994) was used to propose downwelling induced by cold regions of the mantle, a dynamic result first confirmed in non-magnetic convection by Zhang & Gubbins (1996), later in dynamical dynamo runs (Glatzmaier *et al.* 1999; Bloxham 2000; Christensen & Olson 2003), and finally in a solution with narrow downwelling plumes locked to the boundary (Gubbins *et al.* 2007). Another example is the observed switch between steady and oscillatory solutions when the meridional circulation is changed in a kinematic solution (Gubbins & Gibbons 2002; Willis & Gubbins 2004), which led to new interpretation of a reversal in a dynamical dynamo (Sarson & Jones 1999; Sarson 2000). In a more quantitative approach Sarson (2003) has modified a class of flows studied extensively for kinematic dynamo action so that it satisfies the thermal wind equation, a first step towards determining a dynamical dynamo from kinematic solutions that produce magnetic fields of a desired type.

(iv) The kinematic approach amounts to exploring solutions of the induction equation, or finding the modes of the induction operator. The modes could be useful in exploring the full dynamical solution because any candidate magnetic field can be expanded in the set of modes. It remains to be seen how successful this approach will be given the numerical effort required to find the modes in the first place. For example, the Backus dynamo (Backus 1958) is a simple example of a kinematic dynamo with time dependent flow: the same steady flow is switched on and off periodically. The general solution for this time-dependent flow can be represented in terms of modes of the induction equation when the flow is turned on and by the decay modes when the flow is turned off. Each mode decays or grows exponentially with time, so the time dependence can be followed by applying the growth or decay factors and transforming between the two bases each time the flow is switched. The numerical scheme is only efficient when most of the modes decay very quickly and it is only necessary to use a small number of modes. In another example, Melbourne *et al.* (2001) presented a simple dynamical system exhibiting a heteroclinic cycle as a model for geomagnetic reversal behaviour. The system possesses three saddle points and cycles between them, remaining near a saddle for a long time before switching to another saddle. The saddles represent solutions of the induction equation with different symmetry (for example, steady and oscillatory modes) and the transition between them a breakdown from one symmetry to another. The study requires prior knowledge of modes of the induction equation for suitable flows.

Kinematic theory is limited in two major respects: we do not know the flow in the core, and an impossibly large class of flows would need to be explored in order to establish a definitive connection between the fluid flow and the observed field. Nevertheless, generic results can be drawn from a limited study and these may be tested by appropriate dynamical studies.

Recent results from a number of kinematic dynamo studies are based on the flow chosen by Kumar & Roberts (1975). This flow has the advantage of generating a magnetic field with a fourfold symmetry that resembles that of the Earth. The resemblance is fortuitous because the original authors were simply building flows they thought would act as dynamos, guided by the previous attempts of Bullard & Gellman (1954) and Lilley (1970) and the Braginsky theory (Braginsky 1964). The model has convective downwelling on the great circle $\phi = \pm 90^\circ$ that tends to concentrate surface flux; in the core the surface flux is concentrated around the Pacific. This similarity adds real geophysical relevance to a whole class of flows based on the original Bullard–Gellman flow. The flows have been extended in the recent studies of Nakajima & Kono (1991, 1993), Hutcheson & Gubbins (1994), Sarson & Gubbins (1996), Sarson & Busse (1998), Gubbins *et al.* (2000a,b), Gubbins & Gibbons (2002) and Sarson (2003).

The theory and method of solution is described in Section 2. Section 3 reviews the generic results relevant for the Earth's magnetic field. The results are interpreted in terms of dynamo action, field morphology and time dependence in Section 4.

2 THEORY

In the kinematic dynamo problem the fluid velocity $\boldsymbol{v}$ is specified and the magnetic field is governed by the induction equation:

$$\frac{\partial \boldsymbol{B}}{\partial t} = R_m \nabla \times (\boldsymbol{v} \times \boldsymbol{B}) + \nabla^2 \boldsymbol{B}, \tag{1}$$

where $R_m = \mu\sigma\, Vc$ is the dimensionless magnetic Reynolds number, μ the magnetic permeability, σ the electrical conductivity, and c the linear dimension. Eq. (1) is solved in a sphere of radius c with insulating boundary conditions, so that $\boldsymbol{B}$ must match a potential external field at $r = c$.

When $\boldsymbol{v}$ is independent of time solutions of (1) take the form $\boldsymbol{B} = \boldsymbol{B}_0 \exp{(p + i\omega)t}$. The growth rate p and oscillation frequency ω may be found efficiently as an eigenvalue problem. Dynamo action is said to occur if the growth rate $p(R_m) \geq 0$. The critical magnetic Reynolds number R_m^c yields zero net growth in $\boldsymbol{B}$: $p(R_m^c) = 0$. When $\boldsymbol{v}$ is time dependent (1) must be solved by time stepping unless $\boldsymbol{v}$ is periodic in time with period T, when solutions take the form $\boldsymbol{B}_q \exp[qt]$ where $\boldsymbol{B}_q$ is periodic with period T and q is a Floquet parameter. The eigenvalue problem may then be solved efficiently by a few time integrations of one period (Willis & Gubbins 2004).

Many different geometries and different flows have been considered; spherical geometry is the most relevant to the geodynamo and the flows are usually expressed in terms of vector spherical harmonics

$$\boldsymbol{v} = \sum_{lmst} \epsilon_l^{mt} \boldsymbol{t}_l^m + \epsilon_l^{ms} \boldsymbol{s}_l^m, \tag{2}$$

where $\boldsymbol{t}_l^m$, $\boldsymbol{s}_l^m$ are toroidal and poloidal vector spherical harmonics:

$$\boldsymbol{t}_l^{m\{c/s\}} = \nabla \times \left[t_l^m(r) P_l^m(\cos\theta)\{\cos/\sin\}(m\phi)\boldsymbol{e}_r\right], \tag{3}$$

$$\boldsymbol{s}_l^{m\{c/s\}} = \nabla \times \nabla \times \left[s_l^m(r) P_l^m(\cos\theta)\{\cos/\sin\}(m\phi)\boldsymbol{e}_r\right], \tag{4}$$

(r, θ, ϕ) are spherical coordinates, P_l^m are Schmidt-normalized associated Legendre functions, and $\boldsymbol{e}_r$ is the unit radial vector. Flows consistent with convection influenced by rotation are expected to be dominated by symmetry about the equator, which requires the toroidal harmonics to have $l - m$ odd and poloidal harmonics to have $l - m$ even (Gubbins & Zhang 1993). This amounts to invariance under the transformation $\theta \rightarrow \pi - \theta$. Other symmetries have been considered and may prove important in geomagnetic field behaviour. Generated magnetic fields have the same or lower symmetry than the underlying flow. For example, flow with this 'equatorial' symmetry may generate magnetic fields that are either antisymmetric about reflection in the equatorial plane, the so-called dipolar family, or symmetric about reflection in the equatorial plane, the quadrupole family. The different symmetries are usually expressed in terms of the leading harmonic in the poloidal field, $l = 1$, $m = 0$ or $l = 2$, $m = 0$. Solutions with different symmetry are linearly independent in the kinematic problem because the induction eq. (1) is linear; any linear combination is also a solution. The full dynamical dynamo problem is non-linear and solutions may not be combined, but they are separable and may exist in isolation. This adds relevance to the study of independent solutions of the kinematic problem.

The radial functions $t_l^m(r)$ and $s_l^m(r)$ must be chosen to satisfy the boundary conditions and continuity conditions at the origin (although this has not always been followed); they are otherwise arbitrary. Most authors have chosen simple polynomial and trigonometric functions, sometimes modified by a taper function near the boundary. Some authors have used spherical Bessel functions, which amounts to expanding the flow in the natural decay modes of the

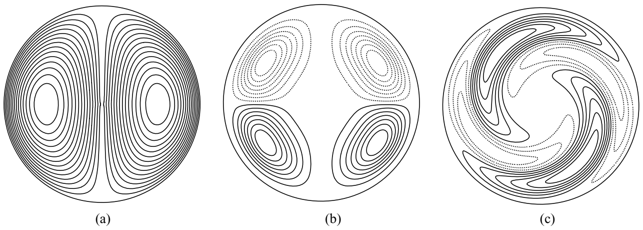

Figure 1. Fluid flow defined by eq. (5). (a) contours of v_ϕ, controlled by parameter ϵ_0, in meridian section (b) streamlines of meridional circulation (ϵ_1) in meridian section (c) streamlines of convection rolls (ϵ_2, ϵ_3) in equatorial section.

sphere, because they optimize the helicity. The wide variety of radial function emphasizes the arbitrary nature of the kinematic problem but it is, in fact, no more or less arbitrary than the use of vector harmonics, which have no better case for admission other than that they satisfy the solenoidal and continuity conditions. We seek robust, generic results that should be independent of the particular choice of radial function, but this can never be guaranteed. Dudley & James (1989) review most of these flows.

The most intensive study of a single class of flows has been conducted for generalizations of the Kumar–Roberts dynamo (Kumar & Roberts 1975) itself a development of the failed Bullard–Gellman dynamo. The flow is defined as:

$$\boldsymbol{v} = \epsilon_0 \boldsymbol{t}_1^0 + \epsilon_1 \boldsymbol{s}_2^0 + \epsilon_2 \boldsymbol{s}_2^{2c} + \epsilon_3 \boldsymbol{s}_2^{2s}, \tag{5}$$

with radial functions defined by

$$\begin{aligned} t_1^0(r) &= r^2(1-r^2), \\ s_2^0(r) &= r^6(1-r^2)^3, \\ s_2^{2c}(r) &= r^4(1-r^2)^2\cos(n\pi r), \\ s_2^{2s}(r) &= r^4(1-r^2)^2\sin(n\pi r). \end{aligned} \tag{6}$$

The first harmonic represents differential rotation about the coordinate axis (which is implicitly assumed to be also the rotation axis), the second meridional circulation, and the last two convective overturn. These three constituents of the flow are shown in Fig. 1; in some sense they are the simplest flows that can generate the basic features of the Earth's magnetic field and mimic convection in a rotating sphere. Bullard & Gellman (1954) used only harmonics $\boldsymbol{t}_1^0$ and $\boldsymbol{s}_2^{2c}$; Lilley (1970) added $\boldsymbol{s}_2^{2s}$ to remove the plane of symmetry found to prevent dynamo action in the Braginsky limit (Braginsky 1964) (we would now say it adds helicity to the flow); and Kumar & Roberts (1975) added $\boldsymbol{s}_2^0$ because it was found to promote steady solutions in mean-field $\alpha\omega$ dynamos (Roberts 1972b). Sarson & Busse (1998) added higher wavenumbers to the convective part ($\boldsymbol{s}_l^m$) in order to study the effect of more convection rolls and non-sectorial ($l \neq m$) behaviour. Sarson (2003) further modified the flow so that it satisfied the thermal wind equation, bringing the flow closer to what might be driven by temperature differences. This involves removing the meridional circulation ($\epsilon_1 = 0$) and adding toroidal harmonics $\boldsymbol{t}_3^{2\{c/s\}}$ based on the radial functions

$$t_3^{2\{s/c\}} = \pm\frac{4}{5}\left(\frac{\mathrm{d}}{\mathrm{d}r} - \frac{3}{r}\right) s_2^{2\{c/s\}}. \tag{7}$$

Initial studies focused on values of the parameters $\{\epsilon_i\}$ close to the asymptotic regime studied by Braginsky (1964), the rather complicated limit $R_m \to \infty$ with $\epsilon_1 R_m$, $\epsilon_2 R_m^{1/2}$, and $\epsilon_3 R_m^{1/2}$ remaining finite (Nakajima & Kono 1991; Hutcheson & Gubbins 1994; Sarson & Gubbins 1996). This allowed comparison with existing solutions for the simpler, axisymmetric, Braginsky mean field equation, identical with the $\alpha\omega$ equation of mean field electrodynamics (Steenbeck *et al.* 1966; Roberts 1972b).

This choice of flow has another advantage for studying the geodynamo: the symmetry of periodic repetition in ϕ (only $m = 2$ terms are present). The present geomagnetic field has approximately this symmetry, and there is palaeomagnetic evidence to suggest that the same symmetry has persisted for a long time. Not all choices of the ϵ_i are independent because of this additional symmetry. The transformations $\phi \to \phi + \pi/2$ and $\phi \to -\phi$ show the equivalence of the four combinations:

$$(\epsilon_0\ \epsilon_1\ \epsilon_2\ \epsilon_3), \quad (\epsilon_0\ \epsilon_1\ -\epsilon_2\ -\epsilon_3), \quad (-\epsilon_0\ \epsilon_1\ -\epsilon_2\ \epsilon_3), \\ (-\epsilon_0\ \epsilon_1\ \epsilon_2\ -\epsilon_3). \tag{8}$$

(Dudley & James 1989). The four different solutions for $\boldsymbol{B}$ separate because of these symmetries, depending on whether they change sign under reflection in the equatorial plane or rotation through an angle π about the coordinate axis. The four symmetries are denoted by their leading poloidal vector spherical harmonic: axial dipole D_a (led by $l = 1, m = 0$), axial quadrupole $Q_a (l = 2, m = 0)$, equatorial dipole $D_e (l = 1, m = 1)$, and equatorial quadrupole $Q_e (l = 2, m = 1)$ [notation of Holme (1997)]. The same symmetries apply to the higher wavenumbers and thermal wind flows studied by Sarson & Busse (1998) and Sarson (2003). Many studies have concentrated on the case $\epsilon_2 = \epsilon_3$ to optimize helicity in the convective overturn. Changing the sign of R_m reverses the flow, so the second of these combines with $R_m \to -\mathrm{R}_m$ to produce the combination $(-\epsilon_0\ -\epsilon_1\ \epsilon_2\ \epsilon_3)$. If we set $\epsilon_2 = \epsilon_3$, we can also restrict R_m to positive values and still explore the full range of dynamo solutions defined by the two parameters ϵ_0 and ϵ_1.

R_m must be defined consistently to compare dynamo action between different flows, particularly when comparing the Braginsky regime with more balanced flows.

The Braginsky regime is completely dominated by differential rotation, so one has to be careful to state whether R_m is based on the small but essential radial flow or the much larger azimuthal flow. In the first comprehensive study of kinematic dynamo action of this class of flows outside the Braginsky regime, Gubbins *et al.* (2000a) defined R_m so that the total kinetic energy of the flow is unity:

$$\int \boldsymbol{v}^2 \mathrm{d}V = \alpha\epsilon_0^2 + \beta\epsilon_1^2 + \gamma\epsilon_2^2 + \delta\epsilon_3^2 = 1, \tag{9}$$

where the scalars $\alpha, \beta, \gamma, \delta$ are integrals of the radial functions (6). The fraction of energy in the meridional circulation is then

$$M = \mathrm{sgn}(\epsilon_1)\beta\epsilon_1^2, \tag{10}$$

and that for differential rotation

$$D = \mathrm{sgn}(\epsilon_0)\alpha\epsilon_0^2. \tag{11}$$

The remaining energy lies in convection or radial overturn

$$C = 1 - |M| - |D|. \tag{12}$$

The entire class of flows is defined by the diamond $|M| + |D| \leq 1$. $D > 0$ gives westward surface flow; $M > 0$ gives surface flow towards the equator and away from the poles.

The Braginsky limit becomes:

$$R_m \to \infty, \quad |D| \to \pm 1, \quad |M| \to 0 \tag{13}$$

in such a way that

$$1 - |D|^2 = K|M|, \tag{14}$$

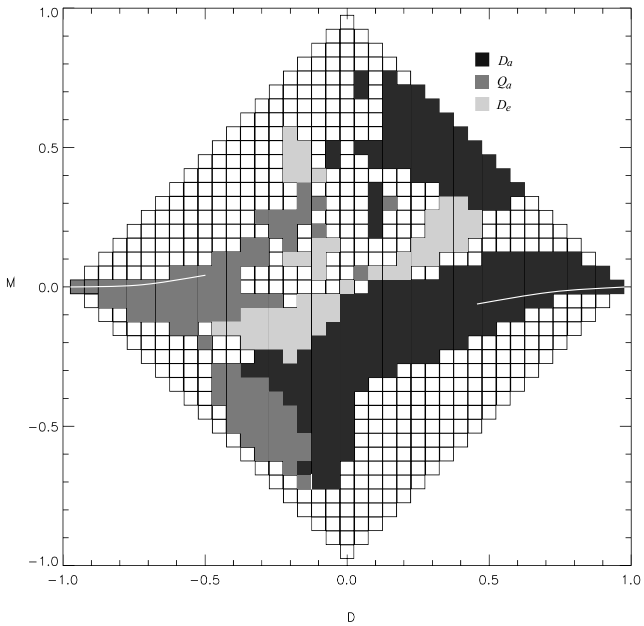

Figure 2. Dynamo action of two-parameter family of flows. Blank squares do not support dynamo action. Greyscale gives solution symmetry with lowest R_m^c. White lines are where oscillatory solutions have been found corresponding to oscillatory solutions in the Braginsky limit. After Gubbins & Gibbons (2002).

where K is a finite non-zero constant. Eq. (13) describes quadratics in (D, M) parameter space (Fig. 2) passing through each of the limit points $D = \pm 1$.

Other special cases of (5) have been the focus of attention, usually with somewhat different radial functions (Dudley & James 1989; Holme 2003). Axisymmetric flows with $m = 0$, on the boundary of the diamond in Fig. 2, cannot generate axisymmetric magnetic fields because of Cowling's theorem but they can generate non-axisymmetric magnetic fields. Solutions have the form $\boldsymbol{B} \propto \exp im\phi$ and each mode can be represented by a sum of harmonics with just one value of m. This makes for a much simplified set of equations and an easy numerical solution, which is why they have received so much attention. The dominant $m = 1$ field is an equatorial dipole. If one wants to fit this to a geodynamo one could rotate the whole dynamo through 90° to give a dominant axial dipole, but the flow would not obey the symmetry expected in a rotating system.

Eq. (1) is solved numerically by expanding $\boldsymbol{v}$, $\boldsymbol{B}$ (both are solenoidal, $\nabla \cdot \boldsymbol{v} = \nabla \cdot \boldsymbol{B} = 0$) in vector spherical harmonics and approximating the radial derivatives by some suitable finite difference or collocation scheme. The resulting algebraic eigenvalue problem is solved by standard methods, the Iteratively Restarted Arnoldi Method (IRAM) of (Lehoucq *et al.* 1998) being the most successful general method available. Dynamo action can never be established rigorously by numerical means. This statement goes beyond the usual cautionary remark for numerical rather than analytical solutions because in practice we increase R_m until p becomes positive or until the numerical scheme is incapable of representing the solution. If no dynamo exists within the accessible range of R_m we still cannot rule out dynamo action at higher R_m. The edges of each dynamo region in Fig. 2, where dynamo action fails, present the most severe numerical convergence problems. At these boundaries R_m^c typically rises dramatically, $\boldsymbol{B}$ becomes spatially complex, and dynamo action is lost with little warning. Further details of the numerical methods are described in Gubbins *et al.* (2000a).

For time-periodic flows the solutions are found by integration in time. Provided we integrate for long enough the fastest growing mode will ultimately dominate (the slowest decaying mode dominates if there are no growing modes). We can do better than this by restarting the time integration after each period T. An arbitrary initial solution is time-stepped for one period, then restarted with a solution orthogonal to the first. Repeated integration and orthogonalization after each cycle soon leads to a set of modes that accurately represents the fastest growing (or slowest decaying) solution. The method is fast and requires very little memory, unlike IRAM, which must store a large banded matrix. This *matrix-free Krylov subspace* method is described further in Willis & Gubbins (2004).

3 RESULTS

3.1 Dynamo action

Dynamo practitioners have two opposing experiences, either that no obvious choice of flow works as a dynamo (viz. Bullard & Gellman 1954; Lilley 1970), or that almost all sufficiently complicated flows act as dynamos e.g. Roberts (1972a). The Kumar–Roberts class of flows were, therefore, studied to determine what proportion act as dynamos. Over half of the flows with $\epsilon_2 = \epsilon_3$ generate magnetic field of one symmetry or another; many generate fields of 2 symmetries or even 3 with different R_m^c; and a few generate two distinct symmetries with identical R_m^c—for example the ones lying on the boundary lines between zones in Fig. 2.

The sides of the diamond in Fig. 2 have $C = 0$ and flows that are axisymmetric. They cannot generate D_a or Q_a fields because of Cowling's theorem, which states that no axisymmetric field can be sustained by dynamo action, but D_e and Q_e fields are possible. None have been found with the original Kumar–Roberts choice of radial functions but similar flows were studied by Bullard & Gubbins (1977) and Dudley & James (1989) using slightly different radial functions. Both found D_e fields for some of their flows. Bullard & Gubbins (1977) noted strongly sheared magnetic fields near the outer boundary with their first choice of flow, which did not produce dynamo action. Adding an outer layer of stagnant fluid did produce dynamo action. The stagnant conducting layer reduced field gradients near the outer boundary, thus reducing energy loss by diffusion. Dudley & James (1989) used very much simpler radial functions and obtained dynamo action without a stagnant layer. Holme (1997) modified the Kumar–Roberts flow by changing the s_2^0 radial function to $r^3(1 - r^2)^2$, a close approximation to the Dudley & James (1989) trigonometric function, and obtained D_e solutions. Love & Gubbins (1996b) addressed the problem of choosing suitable radial functions by developing an optimization technique to find flows that produce smooth, and therefore well converged, magnetic fields. Holme (2003) used an optimization technique to explore the efficiency of radial functions in promoting dynamo action and found a spatial separation of poloidal and toroidal shear helped dynamo action; he concluded the Dudley & James flow is close to optimal.

The line $D = 0$ has purely poloidal motion. It is well known that purely toroidal motion cannot sustain a magnetic field (Bullard & Gellman 1954), and a similar antidynamo theorem has been conjectured for purely poloidal motions; this numerical demonstration shows the conjecture not to be true (Love & Gubbins 1996b). The solution at the centre has no differential rotation and generates a D_e field (Holme 1997). No convincing dynamo exists at $D = M = 0$ with the original Kumar–Roberts flows, although recent exploration has revealed a number of oscillatory D_e and Q_e solutions near the centre of the diamond (Gubbins 2008).

The line $M = 0$ has no meridional circulation; the dynamo studied by Lilley (1970) is on this line close to $D = 1$. Lilley's choice lies just outside the dynamo region, and a tiny change in his flow produces a successful dynamo. Unfortunately, the growing solution he reported was a numerical artefact. Bullard & Gellman (1954) had $M = 0$ with $\epsilon_3 = 0$ and also reported a growing solution that turned out to be a numerical artefact.

3.1.1 *Helicity*

Helicity is thought to promote dynamo action by converting toroidal to poloidal field. Bullard & Gellman (1954) envisaged pushing and twisting of the toroidal field by helical flow to put energy into the dipole field, but by omitting the $\boldsymbol{s}_2^{2s}$ harmonic they lost the helicity. The α-effect of the Braginsky dynamo requires both $\boldsymbol{s}_2^{2c}$ and $\boldsymbol{s}_2^{2s}$ harmonics and is related to the axisymmetric average of the helicity. Pekeris *et al.* (1973), in an early study of a dynamo with harmonics $\boldsymbol{s}_2^{2c}$, $\boldsymbol{t}_2^{2c}$, chose Beltrami flows with $\boldsymbol{v}$ parallel to $\nabla \times \boldsymbol{v}$ in order to maximize the helicity. Beltrami flows have radial functions based on spherical Bessel functions. Nakajima & Kono (1993) made a thorough study of the effect of helicity on kinematic dynamos, including the Pekeris dynamo, and concluded that the dynamo was more efficient for larger mean helicity.

Most studies have concentrated on the case $\epsilon_2 = \epsilon_3$, which optimizes the helicity. Kumar & Roberts (1975) found numerical convergence was best in this case, and Hutcheson & Gubbins (1994) found that when ϵ_2 and ϵ_3 differ by too much the dynamo fails. The flows near the Braginsky limit points $D = \pm 1$ act as $\alpha\omega$ dynamos, the link being formal in the appropriate limit. Flows near the centre line $D = 0$ might be expected to behave like α^2 dynamos, and to some extent they do. Steenbeck & Krause (1969b) [translated in Roberts & Stix (1971)] originally proposed that the Earth had an α^2 dynamo because its field was steady, while the Sun had an $\alpha\omega$ dynamo because its field was oscillatory.

Maximizing the mean helicity does not always lead to enhanced dynamo action. For the Kumar–Roberts dynamo the helicity of the flow depends only on the convective part of the motion and is proportional to the product $\epsilon_2\epsilon_3$. There is an axisymmetric part and a non-axisymmetric part:

$$h = \boldsymbol{v} \cdot \nabla \times \boldsymbol{v} = \epsilon_2\epsilon_3[H_0(D, M) + H_1(D, M)\cos 2\phi]. \qquad (15)$$

Surprisingly, Love & Gubbins (1996a) found that the most efficient dynamo (the one with lowest R_m^c normalized by the kinetic energy) on the $D = 0$ line was not at the centre $M = 0$, where the helicity is a maximum for the kinetic energy available, but at a point where the non-axisymmetric part of the helicity [H_1 in (15)] is a maximum. This appears to hold rather generally, well away from the Braginsky limit. Fig. 3 shows the non-axisymmetric part of the helicity compared to R_m^c for the D_a symmetry solutions. It seems that axisymmetric helicity, in which the flow pushes and twists the toroidal field in the same sense for all ϕ, does not lead to reconnection of the field to reinforce the poloidal field (Love & Gubbins 1996a).

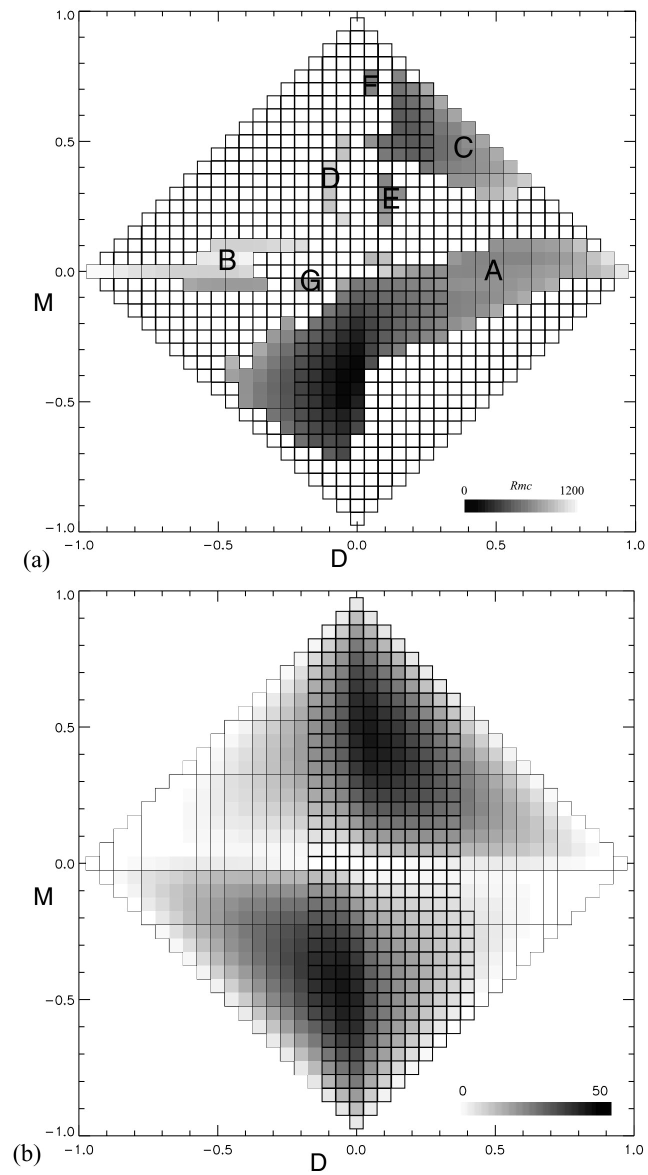

Figure 3. (a) Flows giving dynamo action with D_a symmetry. Letters A–G label distinct regions of dynamo action separated by areas where no dynamos have been found. R_m^c as shown by the grey scale at bottom right. (b) Non-axisymmetric helicity of the flow, $H_1(D, M)$ in (15). Note the correspondence with R_m^c, suggesting H_1 promotes dynamo action. After Gubbins *et al.* (2000a).

3.1.2 *Effect of stagnation points and concentration of magnetic flux on dynamo action*

The boundaries between dynamo and non-dynamo regions in Fig. 2 are usually characterized by a rapidly rising critical magnetic Reynolds number and concentration of magnetic flux into a few isolated spots. Flux concentration is independent of the sign of $\boldsymbol{B}$ and is often enhanced at stagnation points of the flow, where magnetic field may be carried in from many directions and, in some circumstances, is limited only by diffusion. At high R_m the flux is concentrated into narrow zones with diffusion enhanced accordingly. Since the only degree of freedom in this kinematic calculation is to change R_m, there comes a point at which increasing R_m enhances diffusion more rapidly than enhancing the dynamo action, the dynamo fails, and the growth rate becomes a decreasing function of R_m. Stagnation points are, therefore, central to determining the dynamo action. On the surface, stagnation points are identified as centres of upwelling and downwelling; flux tends to be concentrated over downwellings.

3.1.3 *Boundary effects*

A major problem with early searches for kinematic dynamo action lay with the choice of radial function. The work of G. O. Roberts on periodic dynamos in infinite media showed that dynamo action would be possible if the flow took on a cellular form with field regeneration taking place by interaction between cells away from the insulating boundary (Roberts 1972a). This led to the choice of multiple cells in radius, as in Gubbins (1972) and the Kumar–Roberts dynamo [eqs (6) with $n > 1$]. Bullard & Gubbins (1977) identified a current sheet developing near the insulating boundary of many single-cell dynamos and attributed loss of dynamo action to enhanced ohmic diffusion near the boundary. They achieved dynamo action by adding a stagnant layer of fluid around the region of motion; this allows electric currents to flow out of the region where field is generated, reduces the diffusion, and allows dynamo action. There is no hard-and-fast rule about the advantages of a stagnant layer, it depends on whether the field regeneration leads to production of radial current density near an insulating boundary. Changing boundary conditions from insulating to perfectly conducting (where the current density is required to be normal rather than parallel to the boundary) usually improves dynamo action.

Dudley & James (1989) obtained dynamo action with axisymmetric flows based on very simple radial functions. This model has received considerable attention because of its simplicity but numerical convergence in the radial direction is slow, presumably because of enhanced surface currents [although note Livermore & Jackson (2004b) attribute the difference to differences in shear at the origin]. This high sensitivity of dynamo action to changes in radial function is another example of the sudden change from dynamo generation to dynamo failure seen at the edges of dynamo regions in Fig. 2.

The problem of boundary-enhanced diffusion has surfaced more recently with the attempt to obtain dynamo action in the laboratory, where magnetic Reynolds numbers are necessarily restricted to low values and dynamo action must be made as efficient as possible. Kaiser & Tilgner (1999) studied a Ponomarenko dynamo surrounded by stagnant fluid. They found cases where dynamo action was impaired as well as enhanced, but concluded that laboratory models would benefit from leaving some of the fluid stationary. These conclusions were confirmed in a separate study by Stefani *et al.* (2006b).

3.2 Spatial symmetry selection

The geophysically relevant solutions have D_a symmetry and are steady. Other symmetries may be relevant to the Sun, which has an oscillatory magnetic field reversing every 11 yr, or some of the other planets. Magnetic fields of Uranus and Neptune have been discussed in this context by Holme (1997), who found that D_a fields are preferred only in the presence of strong differential rotation. Fig. 1 shows that D_a fields are favoured by $D > 0$. There are two possible explanations of this, described in the next 2 subsections.

3.2.1 Sign of $\alpha\omega$ or dynamo number

Magnetic field generation by $\alpha\omega$ dynamos, whether Braginsky or mean-field, depends on the product of the two magnetic Reynolds numbers, R_α and R_ω, known as the dynamo number (Parker 1979). The $\alpha\omega$ dynamo equations are axisymmetric and attention has focused almost exclusively on D_a and Q_a axisymmetric solutions. The D_a solutions are favoured by positive dynamo numbers, the Q_a solutions by negative dynamo numbers [see Parker (1979) for an extensive discussion]. Parity selection was also resolved by Proctor (1977a,b), who showed further that D_a and Q_a fields would be generated at similar dynamo numbers. The sign of the dynamo number depends simply on the sign of the flow because α is quadratic and ω linear in $\mathbf{v}$. The symmetry relations (8) show that it is possible to change the sign of D (ϵ_0) and α ($\epsilon_2\epsilon_3$) and obtain a dynamo solution with the same R_m^c. All these transformations preserve the dynamo number.

In the Kumar–Roberts dynamo these results are born out by 3-D calculations near the Braginsky limit points. The dynamo number is proportional to the product DM; D_a solutions dominate for $D > 0$, while Q_a solutions dominate for $D < 0$. This reflects the result from Parker's simple $\alpha\omega$ theory, where parity selection is governed by the sign of the product DM. The 3-D results are not fully symmetric with respect to M but become more symmetric when the effective meridional circulation of the full Braginsky theory is used. Fig. 2 shows the crossover of parity at slightly negative values of D. Proctor (1977a) used the solutions of the adjoint $\alpha\omega$ dynamo problem with modified boundary conditions to determine symmetry selection and the critical dynamo number; in the 3-D problem the adjoint induction operator is formed simply by change of sign of $\mathbf{v}$ and change of boundary conditions (Gibson & Roberts 1966), suggesting that a change of sign of both D and M is needed to the change symmetry of the solution. This has been confirmed using flows with stagnant upper layers to reduce and effectively remove the effects of the boundary conditions, which are different for the adjoint problem (Sarson & Gubbins 1996). Fig. 2 confirms the switch from D_a to Q_a with $D \to -$ D, M $\to -M$ near the limit points $D = \pm 1$.

3.2.2 Effects of stagnation points and concentration of magnetic flux on symmetry selection

We have already seen that flux concentration can impair dynamo action. It can also influence symmetry selection. Each symmetry places constraints on the magnetic field, and a symmetry will not be favoured if the flow is such as to generate strong components of field in places forbidden by symmetry. Similarly, a symmetry will be favoured if it allows field components in places where it is concentrated by the flow. Flows that generate more than one symmetry generally do not have strong concentrations of flux.

For example, flows in the centre of the diamond in Fig. 2, those with small D and M, tend to generate strong radial field B_r near the surface at the downwelling limbs of the convection (Gubbins *et al.* 2000b). D_a and Q_e require a change of sign of B_r across the equator, which can only be accommodated with steep field gradients at the equator and high diffusion. Meridional circulation tends to shift surface radial field towards the poles, which inhibits D_e symmetry and favours D_a symmetry. Differential rotation promotes axisymmetric fields and, therefore, favours both D_a and Q_a. The sign of D determines whether surface field is concentrated on the equator, favouring Q_a solutions, or towards the poles, favouring D_a solutions (Gubbins *et al.* 2000b). The result is the same as discussed in the previous section in connection with the sign of the dynamo number; it provides a more geometrical explanation of the effect. Flux concentration is easiest to see in the surface radial field and is the most important for geophysical interpretation, but flux concentration of other components within the core appears to have similar effects (Gubbins *et al.* 2000b).

3.2.3 Preference for axial symmetry?

It is possible the top of the Earth's core is stably stratified, either because the temperature gradient is below the adiabatic gradient or because light elements have accumulated in the upper core. The kinematic results described above show that this may not be detrimental to dynamo action, quite the opposite, but it may have a strong influence on the geomagnetic field at the core surface. A stably stratified region will not be stagnant because horizontal flows are possible; they will be driven by lateral variations in density and by the magnetic force. Love (2000) has explored the effect of toroidal motions in a layer above a kinematic dynamo driven by the Kumar–Roberts flow. His primary aim was to explain the magnetic field of Saturn, which has a high degree of axial symmetry, but his results could also apply to the Earth. He found that simple differential rotation often enhances the axisymmetric part of the field but not always. For the Earth, a layer of purely toroidal flow at the top of the core could improve the match of dynamo model fields with the observed geomagnetic field.

Livermore & Jackson (2006) applied the energy method to a variety of flows that have been studied for kinematic dynamo action. They examine magnetic energy growth and decay for transients for candidate magnetic fields and plot the envelope function, the maximum energy achieved by any field at a particular time. The important fields for dynamo action are the ones for which energy persists the longest, rather than those that grow the most in a short initial burst. They find axisymmetric fields persist the longest, and suggest this is why axisymmetric fields are generally the dominant component of real dynamos. They also suggest that axisymmetric fields may be dominant in a growth phase of a dynamo, such as when the Earth's field is recovering from a reversal (Livermore & Jackson 2004b). They do not give any examples of working dynamos to back up this suggestion. Their results could explain the experiment of Peffley *et al.* (2000), who used flows similar to those of Dudley & James (1989) and found the dominant magnetic modes to be axisymmetric. This was not a dynamo experiment and all the modes decayed, but the dominance of axial symmetry appeared contrary to Cowling's theorem. Tilgner (2002) showed the results were consistent with kinematic theory, but the prevalence of axial symmetry suggests the energy method is effective in predicting the behaviour of real experiments.

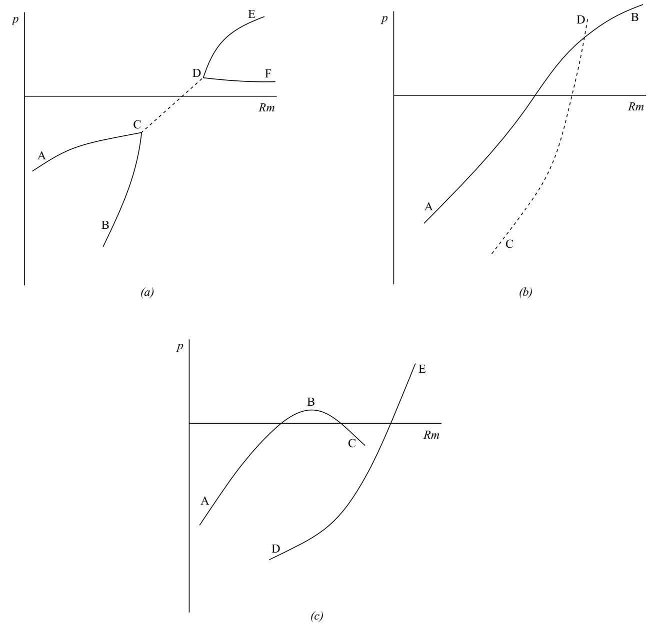

Figure 4. Schematic examples of growth rate curves. Solid lines indicate real growth rates, dotted lines complex growth rates (oscillatory solutions). (a) A pair of real eigenvalues *A* and *B* coalesce to a complex conjugate pair at *C*, which revert to a pair of real at *D*. The physically realisable solution is the one with positive growth rate at lowest R_m, which depends on whether $p \geq 0$. The oscillatory mode is realized in the figure as drawn; any change in fluid velocity that places *C* above, or *D* below, the line $p = 0$ will produce a steady realisable solution. (b) Two separate modes; *AB* is steady and *CD* oscillatory. As drawn *AB* is preferred but a small change in flow can shift *CD* to make it unstable first. (c) *ABC* is steady and preferred as shown. If a small change in flow places *B* below $p = 0$ the oscillatory mode *DF* becomes the only dynamo mode.

3.3 Time dependence

3.3.1 Dynamo waves

Steady flows can only produce steady or oscillatory magnetic fields. Early studies of mean field $\alpha\omega$ dynamos suggested that oscillatory solutions were preferred (Steenbeck & Krause 1969a), but later simple models showed that steady solutions were possible on separation of α and ω in space (Stix 1973; Deinzer *et al.* 1974; Gibbons 1998) or on addition of meridional circulation (Roberts 1972b). Similar results hold for 3-D kinematic dynamos: oscillatory solutions arise when regions of strong poloidal and toroidal components of flow are in the same place, and oscillatory solutions only arise for a very narrow range of meridional circulation around the zero in effective meridional circulation in the Braginsky limit (Gubbins & Gibbons 2002): the zone of oscillatory solutions in Fig. 2 has thickness less than 10^{-2} in M. The absence of oscillatory 3-D solutions is remarkable and in stark contrast to the axisymmetric $\alpha\omega$ results. The explanation is simple: it is easier to separate poloidal and toroidal parts in three dimensions than 2.

The transition from steady to oscillatory solutions can involve either a change of mode or a pair of steady modes coalescing into a complex conjugate pair (eigenvalues of a real operator are either real or occur in complex conjugate pairs). Three possibilities are sketched in Fig. 4. When the same mode changes from real to complex the generated field tends to be similar at certain parts of the cycle. Flux in the oscillatory solutions tends to migrate north-south rather than azimuthally, with flux reversal taking place by new patches forming at the equator (poles) and migrating towards the poles (equator). For some flows both steady and oscillatory solutions are generated with the same critical magnetic Reynolds number.

3.3.2 Time-dependent flow

An interesting result is that time-dependent flows can be better dynamos than steady flows, in the sense that the growth rate is greater than the mean growth rate of the constituent snapshots of the flow (Gog *et al.* 1999; Normand 2003; Willis & Gubbins 2004). This could arise, for example, from movement of the stagnation points to reduce flux concentration and its attendant enhanced diffusion (see Section 3.1.2). It is made possible by non-orthogonality of the modes of the induction equation: if the equation were self-adjoint then varying the flow would not assist dynamo action. With non-orthogonal modes a transient may grow initially but then decay because it is a combination of decaying modes, but as the flow changes so does the spectrum of modes. The field is now a different combination of modes and a new transient may grow, leading to dynamo action. If the modes were orthogonal and all decaying the field would inevitably continue to decay. Livermore & Jackson (2006) used the energy method to explore growth of transients and find them to be quite robust to changes in flow, suggesting they may hold clues to the form of the generated field.

Steady flow is also a great restriction on the possible time behaviour of the magnetic field: it can never produce an Earth-like polarity reversal, for example. Periodic flows are rather special but they allow us to explore some of the possible behaviour of time dependent flow. In particular, it allows us to simulate reversals. If $\boldsymbol{v}$ is periodic in time with period T the solution for $\boldsymbol{B}$ takes the form $\boldsymbol{B}_q(t)\exp[qt]$ with $\boldsymbol{B}_q(t+T)=\boldsymbol{B}_q(t)$. Fourier expansion in time of the periodic quantities is the usual analytical method of solution, but a much more efficient numerical method is to time-step one period for a sequence of orthogonal starting conditions (Willis & Gubbins 2004).

Periodic, time-dependent flows are specified by allowing the velocity parameters D, M to be periodic functions of time, defining a closed curve in the parameter space of Fig. 2. The narrowness of the band of oscillatory solutions means that only very slight changes in fluid velocity are required to change from steady to oscillatory solutions. If the orbit in (D, M)-space is designed to cross or just enter the oscillatory region it is possible to obtain a solution that is almost steady for most of the orbit and oscillates for only a short time. If the period of the orbit is chosen so that the flow remains in the oscillatory region for about half a cycle the field reverses. The solution is periodic with the field remaining almost stationary for most of the cycle and the reversal taking place in a short time.

Stefani & Gerbeth (2005) have studied reversals in mean-field $\alpha\omega$ dynamos with equilibration forced by alpha-quenching (Stefani *et al.* 2006a). They also find reversal behaviour where flows produce both steady and oscillatory kinematic solutions at the same magnetic Reynolds number—places where the growth rate curve for a pair of complex eigenvalues bifurcates into two curves for real eigenvalues as in Fig. 4(a). For high R_m they find these bifurcation points tend to cluster around the zero growth-rate axis, suggesting high R_m-dynamos are prone to reversal behaviour. The mean-field approximation is a limitation and, like any kinematic dynamo, it suffers from the arbitrary choices of α and ω. The relative scarcity of oscillatory solutions in 3-D kinematic dynamos (see Fig. 2) would suggest this argument may be restricted to mean-field dynamos.

4 IMPLICATIONS FOR THE GEODYNAMO AND DYNAMIC MODELS

The kinematic dynamo can help understand the geodynamo in two ways: first, it provides an interpretation of the observed surface magnetic field in terms of the underlying core flow, and secondly it provides physical insights into the dynamo mechanism that can guide further work on the forces driving the flow.

4.1 Main field

The clearest connection between flow and surface field in the dynamo solutions discussed here is concentration of vertical flux by fluid downwelling. This is easy to see for steady flows but harder in dynamic solutions where the flow is often chaotic and varying too much in time for the effect to show up in anything other than a time average. The effect has now been found in a quasi-steady dynamic model dominated by lateral variations in heat flux or temperature at the outer boundary (Gubbins *et al.* 2007; Willis *et al.* 2007; Sreenivasan & Gubbins 2007). These solutions have heat flux boundary conditions determined by lower mantle seismic tomography or a single Y_2^2 spherical harmonic, and narrow downwellings coincide with high radial flux or cold spots on the boundary. In the tomographic case the flux spots match the 4 main lobes of the present geomagnetic field well, indicating a strong mantle influence on the geomagnetic field. The opposite effect, absence of radial surface flux above upwelling, is also observed. The absence of surface flux within the tangent cylinder in the geomagnetic field suggests upwelling there, which places a constraint on the vigour of convection in the whole core (Sreenivasan & Jones 2006). Downwelling near the equator, where with D_a symmetry there is no surface radial field to concentrate, tilts the toroidal field below the surface to produce a typical cloverleaf pattern on the equator. The effect is weak or absent when differential rotation is large, presumably because azimuthal flow dominates the downward flow. Such patterns are often seen in dynamic models and there is a hint of this pattern on the core surface beneath Indonesia (Bloxham & Gubbins 1985), but nothing as strong as is usually seen in the models. This absence may be because of strong azimuthal flow or weak vertical motion near the core mantle boundary resulting from local stratification, as discussed in Section 3.2.3

The primary feature of the geomagnetic field is the dominant axial dipole, which has persisted throughout Earth's history. The kinematic models reported on here require significant differential rotation to produce axial dipole symmetry, solutions with weak differential rotation and meridional circulation being dominated by D_e and Q_e symmetry. Differential rotation tends to produce a large, axisymmetric toroidal field that promotes axisymmetric poloidal fields. D_a symmetry is preferred when the differential rotation leads to surface azimuthal drift in the same sense as the spiralling of the convection rolls. In the Earth the surface drift is predominantly westward, so we should expect a predominantly eastward spiralling, but this is not seen clearly in the shape of the main lobes of the geomagnetic field. This may be because what we observe is a blurred combination of several individual rolls that are obscured by the limited resolution of core field maps, it may be that convection is suppressed near the CMB and we observed the blurred effect of a more complex field at depth, or it may simply be that spiralling is weak under core conditions.

Axial dipole symmetry is also favoured by flux concentration at high latitudes because no sharp field gradients are needed. In dynamic models flux tends to be concentrated outside the tangent cylinder, near 70°N and S, also favouring D_a symmetry. However, the kinematic dynamos discussed here have no inner core yet still lead to flux concentration at high latitudes. There is no reason, therefore, to expect any dramatic change in geomagnetic field morphology in earlier times when the inner core may have been smaller. Dynamical studies tend to confirm this [for example, Bloxham (2000)].

Spiralling of the rolls not only provides the helicity required by the Braginsky theory, it also provides a succession of rolls that overlap with radius [Fig. 1(c)], enabling the reconnection of small scale fields within each roll to reinforce the large scale field, as happens in turbulent or periodic dynamos. Such intuition, based on the Braginsky theory, remains useful for large areas of the parameter space defining the 3-D flows, and is an important aid to understanding dynamo action in general.

The early picture of a geomagnetic field with a dipole moment remaining stationary for several hundred thousand years between polarity reversals has been shown by fine resolution paleointensity studies to be false [e.g. Guyodo & Valet (1999)]: the geomagnetic field strength is continually fluctuating by a large fraction of its maximum value and never remains constant for very long. This suggests the core flow is also continually changing. Kinematic studies show that steady flows make poor dynamos because they contain stagnation points; it is also worth noting that some of the dynamos driven by time-dependent, oscillatory flows studied by Willis & Gubbins (2004) had lower critical magnetic Reynolds numbers than any dynamo driven by a stationary, instantaneous flow in the cycle [see also Gog *et al.* (1999)]. Most dynamic dynamo models have chaotic flows that are highly time dependent and, therefore, avoid this problem: it seems that any sufficiently chaotic and vigorous flow will generate a magnetic field. The mixing properties of these time dependent flows ensure that severe flux concentrations do not arise.

It is worth asking how dynamic solutions avoid severe diffusion arising from flux concentration—does the Lorentz force reduce the flow speeds in these locations or does it change the pattern of flow? In the limited number of studies undertaken it would seem that the flow pattern is changed, moving or removing the stagnation points; the Lorentz force rarely becomes strong enough to oppose the flow directly before diffusion associated with the flux expulsion becomes too large. The dynamo instability appears to be stronger when the system has the extra degrees of freedom associated with a changing flow, as in the dynamical case, as opposed to a fixed flow, as in the kinematic case. The study of dynamo action by steady flows becomes highly relevant if the mantle influences the core flow strongly. The boundary-locked regime of Gubbins *et al.* (2007) was hard to find and only exists for a small range of the accessible parameters. This is partly because increasing the lateral buoyancy parameter, which controls the amplitude of lateral variations of heat flux on the boundary, ultimately causes the dynamo to fail. Usually dynamo failure occurs when lateral heat flux variations become comparable with the mean vertical heat flux, and may be associated with a locked flow that is nearly steady and has stagnation points.

4.2 Secular variation: frozen-flux theory

Ever since the time of Halley our changing magnetic field has been used to infer mass motion inside the Earth. The idea was formalized in Backus' (1968) theory by invoking induction near the core surface and neglecting diffusion. The theory has been used many times in different guises to infer fluid motion at the core surface. Estimates are required of both B_r and its time derivative $\dot{B}_r$ [or a record of $B_r(t)$ over an interval of time] downward continued to the CMB. Dynamo action requires a balance between induction and diffusion, and it is obvious that frozen-flux theory, by setting diffusion to zero, cannot return the flow responsible for dynamo action directly: inferences made about the geodynamo from maps of core motions must be indirect at best. A circular argument underlies our basic estimate of the core's magnetic Reynolds number because it relies on a velocity estimate based on observed secular variation, which in turn relies on neglect of diffusion!

Kinematic dynamos provide many examples where frozen-flux fails. Most obvious are the steady solutions, where surface flow inversions relying on frozen-in fields inevitably yield zero flow. Love (1999) gives examples of kinematic dynamos with slowly varying magnetic fields for which frozen-flux yields completely misleading fields. Kelly (1996) provides examples of time-varying magnetic fields generated by fluid flow in a spherical shell with magnetic field obtained from a kinematic dynamo solution fixed at the base. At time $t = 0$ the flow in the shell jumps from zero to $\boldsymbol{v}$, generating a time-varying magnetic field at the upper surface that is inverted for the flow using frozen-flux theory. Initially the inversion gives a flow that is approximately correct but it weakens with time and eventually reduces to zero as the transients die away and the magnetic field becomes stationary. Stopping the flow at this point generates more transients but now frozen-flux theory yields $-\boldsymbol{v}$ rather than the correct $\boldsymbol{v} = 0$! These examples show that the results from frozen-flux theory must be treated with caution and will depend critically on the time history of the flow.

The problem with Backus' theory is that the limit $\eta \to 0$ is singular: setting $\eta = 0$ is, therefore, likely to yield artificial results. The problem is made clearer by considering the first order correction to the frozen-flux solution, which turns out to depend on the ratio $(\eta/\omega)^{\frac{1}{2}}$ rather than η, where ω is the frequency of time variations of B_r (Braginsky & Le Mouël 1993; Gubbins 1996). The approximation is clearly wrong for steady fields, where $\omega = 0$. The steady motion theorem of Voorhies & Backus (1985), which asserts that flows found by frozen-flux theory are unique provided the flow remains steady, is flawed for the same reason (Gubbins & Kelly 1996). The frozen-flux approximation is only valid if the magnetic field changes sufficiently rapidly in time, yet it is only useful if the flow changes sufficiently slowly in time to allow an estimate to be made.

In practice secular variation must be estimated by differencing magnetic field measurements made over an interval of time sufficiently long to reduce the errors incurred by the differencing—about a decade for ground measurements but significantly less for the data from the new generation of satellites. This defines the shortest time scale that can be studied. We may be lucky in having rapid geomagnetic changes, such as jerks, that appear to be consistent with slower changes in fluid flow (Zatman & Bloxham 1997; Bloxham *et al.* 2002). Success with frozen-flux inversions of dynamical geodynamo simulations could also be attributed to rapid variations in field associated with rather slow changes in flow, perhaps as a result of advection of small scale magnetic field. However, the main evidence for diffusion at the surface of the Earth's core comes from changes in the reverse flux patches in the southern hemisphere during the last century or so, where upwelling appears to bring toroidal flux to the surface (Gubbins 2007). Diffusion may, and probably does, act as strongly elsewhere where there is upwelling but we cannot discriminate between diffusion and induction unless a patch of flux is surounded by a null-flux curve where $B_r = 0$.

4.3 Excursions and reversals

The present fall in dipole moment is related to reversal of flux in the south Atlantic region and is thought by some to be the beginning of a geomagnetic excursion or even a reversal. The present flux reversal is almost certainly caused by expulsion of toroidal field from deeper within the core, which is rarely seen in dynamic models of the geodynamo. It appears similar to the development of a dynamo wave in the Braginsky regime, in which flux reverses near the equator to produce a patch that migrates poleward (Gubbins & Sarson 1994; Gubbins & Gibbons 2002). The present development in the south Atlantic could be modelled as part of a dynamo wave cycle; a change in flow is required to prevent the field from oscillating regularly but the change need only be small in order to produce the desired effect. Consider a flow with parameters on the boundary between oscillatory and steady solutions in Fig. 2, on the line emanating from the $D = 1$ Braginsky limit point. Such a flow generates oscillatory and stationary magnetic fields at the same critical magnetic Reynolds number. Changing the flow slightly favours the steady solution, changing it again will favour the oscillatory solution. By small, slow changes in time it is possible to construct a time-dependent flow that produces reverse flux patches as part of a dynamo wave (or overstability) but reverts to the steady field before progressing far through the wave cycle. Such events may be studied kinematically by constructing time-periodic flows, where the repeat period of the flow is much longer than the oscillation period of the dynamo wave. Leaving the flow in the oscillatory state for longer would simulate an excursion, and leaving it for half a cycle produces a reversal (Willis & Gubbins 2004).

The symmetry of the dynamo equations under change of sign of field has always meant reversed states were possible, the interesting question is how the geodynamo changes from one state to the other. From a dynamic point of view this may be achieved by symmetry breaking, where a solution of one symmetry becomes unstable to a solution of another symmetry. The critical points determining such evolution are those where solutions with more than one symmetry exist, such as the boundaries between preferred symmetries in Fig. 2. For example, flows with $M < 0$ and small D lie close to the boundary between D_a and Q_a preferred solutions. A time-dependent solution with flow in this region would produce a combination of the symmetries, with D_a giving way to Q_a, possibly producing hemispheric oscillations of the sort studied recently in dynamic calculations by Busse & Simitev (2006). A reversed D_a may eventually be established, the transition field indicating the nature of the reversal mechanism. The transition via an oscillatory solution is an alternative symmetry breaking (the symmetry in this case being invariance under translation in time); it seems a more likely candidate for geomagnetic reversals than Q_a symmetry-breaking because it produces systematic VGP paths in the transition field, as is sometimes observed (Love & Mazaud 1997). However, static 'intermediate states' occurring during transition, as have been proposed by Hoffman (2000) and others, might point to a different symmetry; and the same VGP path recorded at all sites would point to a the presence of a D_e mode. Stefani & Gerbeth (2005) model asymmetrical reversals, as proposed by Valet & Meynadier (1993), with a mean-field dynamo, but the observations are disputed (Kok & Tauxe 1996; Mazaud 1996; Laj *et al.* 1996) and it is perhaps too early to read much into the comparison. The kinematic approach to reversals may, however, help interpret observed transition fields when data improve.

5 CONCLUSIONS

Kinematic studies provide a useful bridge between observation and dynamical theory by indicating the type of flow in the core required to produce certain magnetic behaviour. They are limited because the fluid flow is always to some extent arbitrary, and only a small fraction of possible flows can be studied. Nevertheless, some generic conclusions may be drawn about the type of flow and dynamics responsible for generating a magnetic field with some of the properties of the geomagnetic field.

First, dynamo action requires helicity in the form defined by Braginsky's Γ (Braginsky 1964). Furthermore, this helicity is related to the spiralling of convection rolls, which is known to occur in rotating convection but has not yet been observed in the geomagnetic field. The Braginsky limit as originally applied involved implausibly large toroidal fields, but the asymptotics hold well away from the limit and can be usefully applied to more geophysically realistic kinematic dynamos. Magnetic flux is concentrated at stagnation points in the flow, suggesting that the centres of the four main lobes of the geomagnetic field are centres of downwelling.

Secondly, the geomagnetic field's dipolar structure requires a specific combination of westward drift and eastward spiralling, corresponding to a positive dynamo number, as indicated by convection studies. Furthermore, stagnation points that concentrate flux in high latitudes also favour axial dipole fields over axial quadrupole or equatorial dipole fields because the axial dipole requires a change of sign of radial field at the equator.

Finally, although geomagnetic-type reversals in which the field retains the same polarity for long times between rapid reversals are not possible with steady flow, they can be produced by flow that changes very slightly, by less than 0.1 per cent in kinetic energy. The relatively infrequent nature of reversals and absence of oscillations is attributed to the spatial separation of toroidal and poloidal fields, the latter being strongest at high and low latitudes and the former, while not directly observed, being probably strongest in mid-latitudes.

ACKNOWLEDGMENTS

This work was partially supported by NERC consortium grant O/2001/00668. The author would like to thank the Shanghai Astronomical Observatory for their support and hospitality while finalizing this paper.

REFERENCES

Aubert, J., Amit, H. & Hulot, G., 2007. Detecting thermal boundary control in surface flows from numerical dynamos, *Phys. Earth planet. Int.,* **160,** 143–156.

Backus, G.E., 1958. A class of self-sustaining dissipative spherical dynamos, *Ann. Phys.,* **4,** 372–447.

Bloxham, J., 2000. Sensitivity of the geomagnetic axial dipole to thermal core-mantle interactions, *Nature,* **405,** 63–65.

Bloxham, J. & Gubbins, D., 1985. The secular variation of the Earth's magnetic field, *Nature,* **317,** 777–781.

Bloxham, J., Zatman, S. & Dumberry, M., 2002. The origin of geomagnetic jerks, *Nature,* **420,** 65–68.

Braginsky, S.I., 1964. Kinematic models of the Earth's hydromagnetic dynamo, *Geomagnetism i Aeronomiya Geomagnetism and Aeronomy,* **4,** 572–583, English translation.

Braginsky, S.I. & Le Mouël, J.-L., 1993. Two-scale model of a geomagnetic field variation, *Geophys. J. Int.,* **112,** 147–158.

Bullard, E.C. & Gellman, H., 1954. Homogeneous dynamos and terrestrial magnetism, *Phil. Trans. R. Soc. Lond., A,* **247,** 213–278.

Bullard, E.C. & Gubbins, D., 1977. Generation of magnetic fields by fluid motions of a global scale, *Geophys. Astrophys. Fluid Dyn.,* **8,** 43–56.

Busse, F.H., 1970. Thermal instabilities in rotating systems, *J. Fluid Mech.,* **44,** 444–460.

Busse, F.H. & Simitev, R.D., 2006. Parameter dependences of convection-driven dynamos in rotating spherical fluid shells, *Geophys. Astrophys. Fluid Dyn.,* **100,** 341–361.

Christensen, U.R. & Olson, P., 2003. Secular variation in numerical geodynamo models with lateral variations of boundary heat flow, *Phys. Earth planet. Int.,* **138,** 39–54.

Deinzer, W., von Kusserov, H. & Stix, M., 1974. Steady and oscillatory $\alpha\omega$ dynamos, *Astron. Astrophys.*, **36,** 69–78.

Dudley, M.L. & James, R.W., 1989. Time dependent dynamos with stationary flows, *Proc. R. Soc.,* **425,** 407–429.

Elsasser, W.M., 1946. Induction effects in terrestrial magnetism: Part I. Theory, *Phys. Rev.,* **69,** 106–116.

Gibbons, S., 1998. The Parker-Levy reversal mechanism, *Phys. Earth planet. Int.,* **106,** 129–137.

Gibson, R.D. & Roberts, P.H., 1966. Some comments on the theory of homogeneous dynamos, in *Magnetism and the Cosmos*, pp. 108–120, eds Hindmarsh, W., Lowes, F.H., Roberts, P.H. & Runcorn, S.K., Oliver and Boyd, Edinburgh.

Glatzmaier, G.A. & Roberts, P.H., 1995. A three-dimensional convective dynamo solution with rotating and finitely conducting inner core and mantle, *Phys. Earth planet. Int.,* **91,** 63–75.

Glatzmaier, G.A., Coe, R.S., Hongre, L. & Roberts, P.H., 1999. The role of the Earth's mantle in controlling the frequency of geomagnetic reversals, *Nature,* **401,** 885–890.

Gog, J.R., Oprea, I., Proctor, M.R.E. & Rucklidge, A.M., 1999. Destabilisation by noise of transverse perturbations to heteroclinic cycles: a simple model and an example from dynamo theory, *Proc. R. Soc.,* **A455,** 4205–4222.

Gubbins, D., 1972. Kinematic dynamos and geomagnetism, *Nature,* **238** PS, 119–121.

Gubbins, D., 1996. A formalism for the inversion of geomagnetic data for core motions with diffusion, *Phys. Earth planet. Int.,* **98,** 193–206.

Gubbins, D., 2007. Geomagnetic constraints on stratification at the top of Earth's core, *Earth Planets &Space,* **59,** 661–664.

Gubbins, D., 2008. Kinematic dynamo action in a sphere: effects of weak differential rotation and meridional circulation, *Geophys. Astrophys. Fluid Dyn.,* submitted.

Gubbins, D. & Gibbons, S., 2002. Kinematic dynamo action in a sphere. III: dynamo waves, *Geophys. Astrophys. Fluid Dyn.,* **96,** 481–498.

Gubbins, D. & Kelly, P., 1996. A difficulty with using the frozen flux hypothesis to find steady core motions, *Geophys. Res. Lett.,* **23,** 1825–1828.

Gubbins, D. & Sarson, G., 1994. Geomagnetic reversal transition paths from a kinematic dynamo model, *Nature,* **368,** 51–55.

Gubbins, D. & Zhang, K., 1993. Symmetry properties of the dynamo equations for paleomagnetism and geomagnetism, *Phys. Earth planet. Int.,* **75,** 225–241.

Gubbins, D., Barber, C.N., Gibbons, S. & Love, J.J., 2000a. Kinematic dynamo action in a sphere: I. Effects of differential rotation and meridional circulation on solutions with axial dipole symmetry, *Proc. R. Soc.,* **456,** 1333–1353.

Gubbins, D., Barber, C.N., Gibbons, S. & Love, J.J., 2000b. Kinematic dynamo action in a sphere: II. Symmetry selection, *Proc. R. Soc.,* **456,** 1669–1683.

Gubbins, D., Willis, A.P. & Sreenivasan, B., 2007. Correlation of Earth's magnetic field with lower mantle thermal and seismic structure, *Phys. Earth planet. Int.,* **162,** 256–260.

Guyodo, Y. & Valet, J.-P., 1999. Global changes in intensity of the Earth's magnetic field during the past 800 kyr, *Nature,* **399,** 249–252.

Herzenberg, A., 1958. Geomagnetic dynamos, *Phil. Trans. R. Soc. Lond.,* **250,** 543–583.

Hoffman, K.A., 2000. Temporal aspects of the last reversal of Earth's magnetic field, *Phil. Trans. R. Soc. Lond.,* **358,** 1181–1190.

Holme, R., 1997. Three-dimensional kinematic dynamos with equatorial symmetry: application to the magnetic fields of uranus and neptune, *Phys. Earth planet. Int.,* **102,** 105–122.

Holme, R., 2003. Optimised axially-symmetric kinematic dynamos, *Phys. Earth planet. Int.,* **140,** 3–11.

Hutcheson, K.A. & Gubbins, D., 1994. Kinematic magnetic field morphology at the core mantle boundary, *Geophys. J. Int.,* **116,** 304–320.

Jones, C.A., 2000. Convection-driven geodynamo models, *Proc. R. Soc.,* **358,** 873–897.

Kaiser, R. & Tilgner, A., 1999. Kinematic dynamos surrounded by a stationary conductor, *Phys. Rev. E,* **60,** 2949–2952.

Kelly, P., 1996. The time-averaged paleomagnetic field and secular variation, *PhD thesis*, University of Leeds, Leeds.

Kok, Y.S. & Tauxe, L., 1996. Saw-toothed pattern of relative paleointensity records and cumulative viscous remanence.

Kumar, S. & Roberts, P.H., 1975. A three-dimensional kinematic dynamo, *Proc. R. Soc.,* **344,** 235–258.

Laj, C., Kissel, C., Garnier, F. & HerreroBervera, E., 1996. Relative geomagnetic field intensity and reversals for the last 1.8 my from a central equatorial Pacific core, *Geophys. Res. Lett.,* **23,** 3393–3396.

Lehoucq, R.B., Sorensen, D.C. & Yang, C., 1998. *ARPACK USERS GUIDE: Solution of Large Scale Eigenvalue Problems by Implicitly Restarted Arnoldi Methods*, SIAM, Philadelphia, PA.

Lilley, F.E.M., 1970. On kinematic dynamos, *Proc. R. Soc.,* **316,** 153–167.

Livermore, P.W. & Jackson, A., 2004a. On magnetic energy instability in spherical stationary flows, *Proc. R. Soc.,* **460,** 1453–1476.

Livermore, P.W. & Jackson, A., 2004b. Preferential axisymmetric field growth in kinematic geodynamo models, *Geophys. Res. Lett.,* **31,** L22604.

Livermore, P.W. & Jackson, A., 2006. Transient magnetic energy growth in spherical stationary flows, *Proc. R. Soc.,* **462,** 2457–2479.

Love, J.J., 1999. A critique of frozen-flux inverse modelling of a nearly steady geodynamo, *Geophys. J. Int.,* **138,** 353–365.

Love, J.J., 2000. Statistical assessment of preferred transitional VGP longitudes based on palaeomagnetic lava data, *Geophys. J. Int.,* **140,** 211–221.

Love, J. & Gubbins, D., 1996a. Optimized kinematic dynamos, *Geophys. J. Int.,* **124,** 787–800.

Love, J. & Gubbins, D., 1996b. Dynamos driven by poloidal flows exist, *Geophys. Res. Lett.,* **23,** 857–860.

Love, J. & Mazaud, A., 1997. A database for the Matuyama-Brunhes magnetic reversal, *Phys. Earth planet. Int.,* **103,** 207–245.

Mazaud, A., 1996. 'Sawtooth' variation in magnetic intensity profiles and delayed acquisition of magnetization in deep sea cores, *Earth planet. Sci. Lett.,* **139,** 379–386.

Melbourne, I., Proctor, M.R.E. & Rucklidge, A.M., 2001. A heteroclinic model of geodynamo reversals and excursions, in *Dynamo and Dynamics, A Mathematical Challenge*, pp. 363–370,Chossat, P., Armbruster, D. & Oprea, I., Kluwer, Dordrecht.

Nakajima, T. & Kono, M., 1991. Kinematic dynamos associated with large scale fluid motions, *Geophys. Astrophys. Fluid Dyn.,* **60,** 177–209.

Nakajima, T. & Kono, M., 1993. Effect of helicity on the efficiency of laminar kinematic dynamos, *J. Geomagn. Geoelectr.,* **45,** 1575–1589.

Normand, C., 2003. Ponomarenko dynamo with time-periodic flow, *Phys. Fluids,* **15,** 1606–1611.

Olson, P., Christensen, U. & Glatzmaier, G., 1999. Numerical modeling of the geodynamo: mechanisms of field generation and equilibration, *J. geophys. Res.,* **104,** 10 383–10 404.

Parker, E.N., 1979. *Cosmical Magnetic Fields: Their Origin and Their Activity*, Clarendon Press, Oxford.

Peffley, N., Cawthorne, A. & Lathrop, D., 2000. Toward a self-generating magnetic dynamo: the role of turbulence, *Phys. Rev. E,* p. 61.

Pekeris, C.L., Accad, Y. & Shkoller, B., 1973. Kinematic dynamos and the Earth's magnetic field, *Phil. Trans. R. Soc. Lond.,* A, **275,** 425–461.

Proctor, M.R.E., 1977a. On the eigenvalues of kinematic α-effect dynamos, *Astron. Nachr.*, **298,** 19–25.

Proctor, M.R.E., 1977b. The role of mean circulation in parity selection by planetary magnetic fields, *Geophys. Astrophys. Fluid Dyn.*, **8,** 311–324.

Rau, S., Christensen, U., Jackson, A. & Wicht, J., 2000. Core flow inversion tested with numerical dynamo models, *Geophys. J. Int.,* **141,** 485–497.

Roberts, P.H., 1968. On the thermal instability of a self-gravitating fluid sphere containing heat sources, *Phil. Trans. R. Soc. Lond.,* **A263,** 93–117.

Roberts, G.O., 1972a. Spatially periodic dynamos, *Phil. Trans. R. Soc. Lond.,* **266,** 535–558.

Roberts, P.H., 1972b. Kinematic dynamo models, *Phil. Trans. R. Soc. Lond.,* **271,** 663–697.

Roberts, P.H. & Scott, S., 1965. On the analysis of the secular variation. A hydromagnetic constraint: I. Theory, *J. Geomagn. Geoelectr.,* **17,** 137–151.

Roberts, P.H. & Stix, M., 1971. *The Turbulent Dynamo: A Translation of a Series of Papers* by F. Krause, K.-H. Rädler and M. Steenbeck, Tech. Note 60, NCAR, Boulder, Colorado.

Sarson, G.R., 2000. Reversal models from dynamo calculations, *Phil. Trans. R. Soc. Lond.,* **358,** 921–942.

Sarson, G.R., 2003. Kinematic dynamos driven by thermal-wind flows, *Proc. R. Soc.,* **459,** 1241–1259.

Sarson, G.R. & Busse, F.H., 1998. The kinematic dynamo action of spiralling convective flows, *Geophys. J. Int.,* **133,** 140–158.

Sarson, G. & Gubbins, D., 1996. Three-dimensional kinematic dynamos dominated by strong differential rotation, *J. Fluid Mech.,* **306,** 223–265.

Sarson, G.R. & Jones, C.A., 1999. A convection driven geodynamo reversal model, *Phys. Earth planet. Int.,* **111,** 3–20.

Sreenivasan, B. & Gubbins, D., 2008. Dynamos with weakly convecting outer layers: implications for core-boundary locking, *Geophys. Astrophys. Fluid Dyn.,* in press.

Sreenivasan, B. & Jones, C., 2006. Azimuthal winds, convection and dynamo action in the polar regions of planetary cores, *Geophys. Astrophys. Fluid Dyn.,* **100,** 319–339.

Steenbeck, M. & Krause, F., 1969a. Zur dynamotheorie stellarer und planetarer magnetfelder I. berechnung sonnenähnlicher wechselfeldgeneratoren, *Astron. Nachr.,* **291,** 49–84.

Steenbeck, M. & Krause, F., 1969b. Zur dynamotheorie stellarer und planetarer magnetfelder II., *Astron. Nachr.*, **291,** 271–286.

Steenbeck, M., Krause, F. & Rädler, K.-H., 1966. A calculation of the mean emf in an electrically conducting fluid in turbulent motion under the influence of coriolis forces, *Z. Naturforsch.,* **21,** 369–376.

Stefani, F. & Gerbeth, G., 2005. Asymmetric polarity reversals, bimodal field distribution, and coherence resonance in a spherically symmetric mean-field dynamo model, *Phys. Rev. Lett.,* **94,** 184506.

Stefani, F., Gerbeth, G., Gunther, U. & Xu, A., 2006a. Why dynamos are prone to reversals, *Earth planet. Sci. Lett.,* **243,** 828–840.

Stefani, F., Xu, M., Gerbeth, G., Ravelet, R., Chiffaudel, A., Daviaud, F. & Leorat, J., 2006b. Ambivalent effects of added layers on steady kinematic dynamos in cylindrical geometry: application to the VKS experiment, *Europ. J. Mech. B-Fluids,* **25,** 894–908.

Stix, M., 1973. Spherical $\alpha\omega$ dynamos by a variational method, *Astron. Astrophys.,* **24,** 275–281.

Tilgner, A., 2002. Onset of dynamo action in an axisymmetric flow, *Phys. Rev. E,* **66,** 017304.

Valet, J.P. & Meynadier, L., 1993. Geomagnetic-field intensity and reversals during the past 4 million years, *Nature,* **366,** 234–238.

Voorhies, C.V. & Backus, G.E., 1985. Steady flows at the top of the core from geomagnetic field models: the steady motions theorem, *Geophys. Astrophys. Fluid Dyn.,* **32,** 163–173.

Willis, A.P. & Gubbins, D., 2004. Kinematic dynamo action in a sphere: effects of periodic time-dependent flows on solutions with axial dipole symmetry, *Geophys. Astrophys. Fluid Dyn.,* **98,** 537–554.

Willis, A.P., Sreenivasan, B. & Gubbins, D., 2007. Thermal core-mantle interaction: exporing regimes for 'locked' dynamo action, *Phys. Earth Planet. Int.,* **165,** 83–92.

Zatman, S. & Bloxham, J., 1997. Torsional oscillatoins and the magnetic field within the Earth's core, *Nature,* **388,** 760–763.

Zhang, K., 1999. Nonlinear magnetohydrodynamic convective flows in the Earth's fluid core, *Phys. Earth planet. Int.,* **111,** 93–105.

Zhang, K.-K. & Busse, F.H., 1990. Generation of magnetic fields by convection in a rotating spherical fluid shell of infinite Prandtl number, *Phys. Earth planet. Int.,* **59,** 208–222.

Zhang, K. & Gubbins, D., 1996. Convection in a rotating spherical fluid shell with an inhomogeneous temperature boundary condition at finite Prandtl number, *Phys. Fluids,* **8,** 1141–1148.